

Fast and efficient adsorptive removal of manganese (II) from aqueous solutions using malicorium magnetic nanocomposites

Sahar Hafeznejhad and Farid Moeinpour*

Department of Chemistry, Bandar Abbas Branch, Islamic Azad University, Bandar Abbas 7915893144, Iran

Received August 2015; Accepted January 2016

ABSTRACT

Malicorium supported $\text{Ni}_{0.5}\text{Zn}_{0.5}\text{Fe}_2\text{O}_4$ magnetic nanoparticles were synthesized by a low-cost, simple, and environmentally benign procedure. The adsorbent was characterized by several methods including X-ray diffraction (XRD), scanning electron microscopy (SEM) and Fourier transform infrared spectroscopy (FT-IR). Then, the potential of malicorium supported $\text{Ni}_{0.5}\text{Zn}_{0.5}\text{Fe}_2\text{O}_4$ magnetic nanoparticles was investigated for adsorption of Manganese (II). The effect of different parameters including contact time, pH, adsorbent dosage and initial Mn (II) concentration on the Mn (II) removal yield was studied. The experimental data were fitted well with the Langmuir isotherm model. The maximum monolayer adsorption capacity based on Langmuir isotherm is 90.91 mg g^{-1} . The prepared magnetic adsorbent can be well dispersed in the aqueous solution and easily separated from the solution with the aid of an external magnet after adsorption. The process for purifying water treatment presented here is clean and safe using the magnetic nanoparticles. Therefore, this adsorbent was considered to be applicable for managing water pollution caused by Mn (II) ions.

Keywords: Adsorption; Mn (II) ions; $\text{Ni}_{0.5}\text{Zn}_{0.5}\text{Fe}_2\text{O}_4$; Malicorium

INTRODUCTION

Adsorption was established as an important and economically practical treatment technology for removing the Mn (II) ions from water and wastewater. Activated carbon is usually used adsorbent for the removal of Mn (II) ions from aqueous solution. Despite the abundance applications of activated carbon, its uses are sometimes limited due to its high cost and also for loss during its re-formation [1-3]. Therefore, the researchers are on the search for new low-cost substitute adsorbents for the water pollution control, especially, where cost acts an important role. Much efforts have

been done towards the development of another adsorbents that are effective and low-cost. They can be produced from a wide diversity of raw materials, which are abundant and have high carbon and low inorganic content. Owing to the low cost and high accessibility of these materials, it is not essential to have complex regeneration processes. Such low cost adsorption methods have attracted many researchers. Often, the adsorption capabilities of such adsorbents are not large, therefore the study and investigation of more and more new adsorbents are still under development. Several different

*Corresponding author: f.moeinpour@gmail.com;
fmoeinpour52@iauba.ac.ir

adsorbents have been used for removal of manganese ions: clay [4], activated carbon [5], Tamarindus indica fruit nut shells [6], volcanic ashes [7] and glycine modified chitosan resin [8]. In recent years, due to economic problems, creating a cheap and efficient alternative methods of wastewater treatment instead of expensive and inefficient methods is of great importance. One of the most efficient, technical and economic methods in this context, is the use of magnetic adsorbent. These adsorbents have magnetic properties and by using an external magnetic field can be easily separated from the solution. In the magnetic separation, high costs of separation, such as centrifugation and filtration are not included [9]. Extensive researches in the field of magnetization of materials such as chitosan [10], silica [11], polymer [12] and activated carbon [13] have been conducted for water contaminants removal. The use of this property in the nanoparticles, due to their high specific surface area and adsorption capacity is very good [14-16]. Nickel-Zinc ferrites have drawn noticeable consideration of researchers as a result of their remarkable magnetic properties, large permeability, and very high electrical resistivity [17]. They have an extensive potential applications such as high-density information storage devices, microwave devices, transformer cores, magnetic fluids, etc. [18]. The use of activated carbon to remove chlorine, separating gases and air pollution treatment, recycling of heavy metals from aqueous solutions has many applications. But because of the high cost, other options have been suggested as an alternative.

In this context, we became interested to investigate the capability of the surface modified $\text{Ni}_{0.5}\text{Zn}_{0.5}\text{Fe}_2\text{O}_4$ magnetic nanoparticles with malicorium ($\text{Ni}_{0.5}\text{Zn}_{0.5}\text{Fe}_2\text{O}_4/\text{M}$) as a low-cost adsorbent for removal of Mn (II) ions from

aqueous solution and also to study the adsorption mechanism of Mn (II) ions onto this adsorbent. For this purpose, a set of batch adsorption experiments (pH, contact time, adsorbent dosage and initial Mn (II) ions concentration, on the Mn (II) ions removal using this adsorbent) were carried out at optimum conditions. The characterization of the adsorbent was described by FT-IR, XRD and SEM analyses.

EXPERIMENTAL

Materials

Analytical-grade salt $\text{MnCl}_2 \cdot 4\text{H}_2\text{O}$ was obtained from Merck. A 1000 mg/L stock solution of the salt was prepared in deionized water. All working solutions were made by consecutive diluting method with deionized water. Deionized water was prepared using a Millipore Milli-Q (Bedford, MA) water purification system. All reagents ($\text{FeCl}_3 \cdot 6\text{H}_2\text{O}$, ZnCl_2 and $\text{NiCl}_2 \cdot 6\text{H}_2\text{O}$, NaOH and HNO_3) used in the study were of analytical grade and purchased from Aldrich. X-ray diffraction analysis (XRD) was carried out using a PAN analytical X'Pert Pro X-ray diffractometer. Surface morphology and particle size were investigated by a Hitachi S-4800 SEM instrument. FT-IR spectra were determined as KBr pellets on a Bruker model 470 spectrophotometer. All the metal ion concentrations were measured with a Varian AA240FS atomic absorption spectrophotometer.

Synthesis of $\text{Ni}_{0.5}\text{Zn}_{0.5}\text{Fe}_2\text{O}_4/\text{M}$

$\text{Ni}_{0.5}\text{Zn}_{0.5}\text{Fe}_2\text{O}_4/\text{M}$ nanocomposites were synthesized based on the reported method [19]. The solution of metallic salts FeCl_3 (160 mL, 1 M), NiCl_2 (40 mL, 1M) and ZnCl_2 (40 mL, 1M) was poured as quickly as possible into the boiling alkaline solution [NaOH (1000 mL, 1M)] under vigorous stirring. Then about 5 g ground malicorium fragments were added under

constant stirring. The solution was cooled and continuously stirred for 90 min. The resulting material was then separated from the solution by centrifugation.

Adsorption experiments

Batch adsorption of manganese ions onto the adsorbent ($\text{Ni}_{0.5}\text{Zn}_{0.5}\text{Fe}_2\text{O}_4/\text{M}$) was investigated in aqueous solutions under various operating conditions viz. pH 2–7, at a temperature of 298 K, for an initial Mn (II) ion concentration of 5 mgL^{-1} . About 0.30g adsorbent was added to 50 mL of manganesechloride solution (5 mgL^{-1}). Then the mixture was agitated on a shaker at 250 rpm. The initial pH values of the manganese solutions were adjusted from 2 to 7 with $0.1 \text{ mol L}^{-1} \text{ HNO}_3$ or $0.1 \text{ mol L}^{-1} \text{ NaOH}$ solutions using a pH meter. After equilibrium, the samples were centrifuged and the adsorbent ($\text{Ni}_{0.5}\text{Zn}_{0.5}\text{Fe}_2\text{O}_4/\text{M}$) were removed magnetically from the solution. The Mn (II) concentration in the supernatant was measured by flame atomic absorption spectrometer. The effects of several parameters, such as contact time, initial concentration, pH and adsorbent dose on extent of adsorption of Mn (II) were investigated.

The Mn (II) removal percentage was calculated as Eq. (1):

$$\% \text{Removal} = \frac{C_0 - C_t}{C_0} \times 100 \quad (1)$$

where C_0 and C_t (mgL^{-1}) are the concentration of Mn (II) in the solution at initial and equilibrium time, respectively.

The amount of Mn (II) adsorbed (Q_e) was calculated using the Eq. (2):

$$Q_e = \frac{(C_0 - C_e)V}{m} \quad (2)$$

where C_0 and C_e are the initial and equilibrium concentrations of Mn (II) (mgL^{-1}), m is the mass of adsorbent (g), and V is the volume of solution (L).

Adsorption Isotherms

Adsorption isotherms were obtained by using 0.30g of adsorbent and 50 mL of Mn (II) solution with different concentrations ($50\text{--}600 \text{ mg L}^{-1}$) at 298 K. These solutions were buffered at an optimum pH ($\text{pH} = 6$) for adsorption and agitated on a shaker at 250 rpm until they reached adsorption equilibrium (30 min). The quantity of Mn (II) adsorbed was derived from the concentration change.

RESULTS AND DISCUSSION

Characterization of $\text{Ni}_{0.5}\text{Zn}_{0.5}\text{Fe}_2\text{O}_4/\text{M}$ magnetic nanoparticles

$\text{Ni}_{0.5}\text{Zn}_{0.5}\text{Fe}_2\text{O}_4$ nanocrystallites were prepared according to the reported procedure by D. Zins [19]. $\text{Ni}_{0.5}\text{Zn}_{0.5}\text{Fe}_2\text{O}_4/\text{M}$ nanocrystallites were characterized by FT-IR (Figure 1), XRD (Figure 2) and SEM (Figure 3). FT-IR spectra of $\text{Ni}_{0.5}\text{Zn}_{0.5}\text{Fe}_2\text{O}_4$, $\text{Ni}_{0.5}\text{Zn}_{0.5}\text{Fe}_2\text{O}_4/\text{M}$ and M are compared in Figure 1. In the FT-IR spectrum of $\text{Ni}_{0.5}\text{Zn}_{0.5}\text{Fe}_2\text{O}_4/\text{M}$ (Figure 1(A)), much of the bands of $\text{Ni}_{0.5}\text{Zn}_{0.5}\text{Fe}_2\text{O}_4$ (Figure 1(C)) and M (Figure 1(B)) with a slight shift for some of them, are distinct, which shows M has been supported well on the $\text{Ni}_{0.5}\text{Zn}_{0.5}\text{Fe}_2\text{O}_4$. The bands in the low-frequency region ($1000\text{--}500 \text{ cm}^{-1}$) caused by iron oxide framework, which is in accordance to the magnetite spectrum. The peak at 1440.85 cm^{-1} is related to Fe – O bond [20]. In Figure 1A presence of – OH stretching mode is evident by the peak close to 3446 cm^{-1} . To verify the Ni-Zn ferrite formation in the prepared magnetic nanoparticles, the XRD pattern of the sample was investigated. The XRD patterns (Figure 2) show that $\text{Ni}_{0.5}\text{Zn}_{0.5}\text{Fe}_2\text{O}_4$ nanoparticles have the spinel framework, with all the main peaks compatible the $\text{Ni}_{0.5}\text{Zn}_{0.5}\text{Fe}_2\text{O}_4$ standard pattern (JCPDS 08-0234). The particle size of adsorbent was investigated by SEM technique. The SEM photograph of sample

(Figure 3) shows average size of $\text{Ni}_{0.5}\text{Zn}_{0.5}\text{Fe}_2\text{O}_4/\text{M}$ is approximately less than 100 nm.

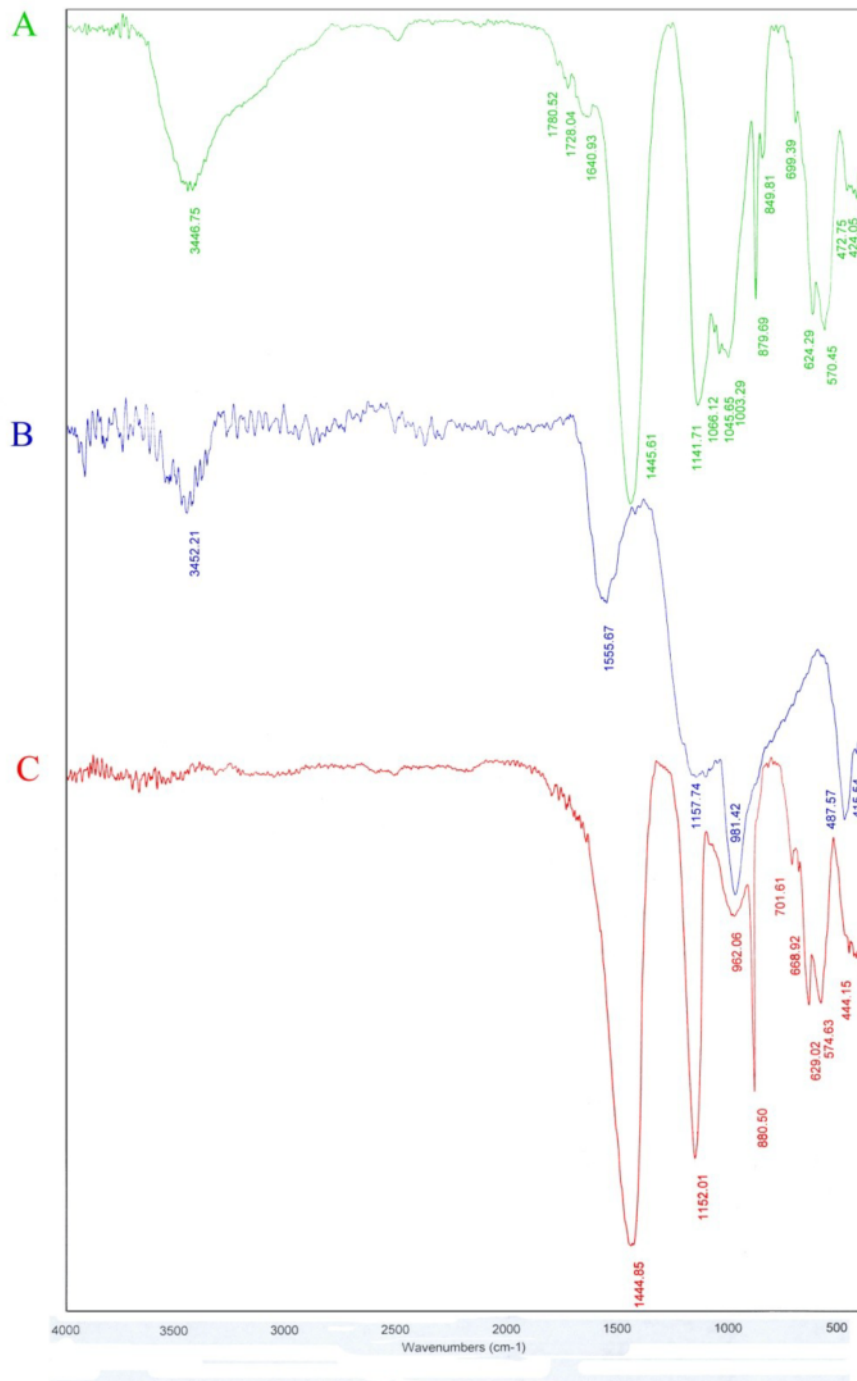


Fig. 1. The FTIR spectra of: (a) $\text{Ni}_{0.5}\text{Zn}_{0.5}\text{Fe}_2\text{O}_4/\text{M}$; (b) M; (c) $\text{Ni}_{0.5}\text{Zn}_{0.5}\text{Fe}_2\text{O}_4$.

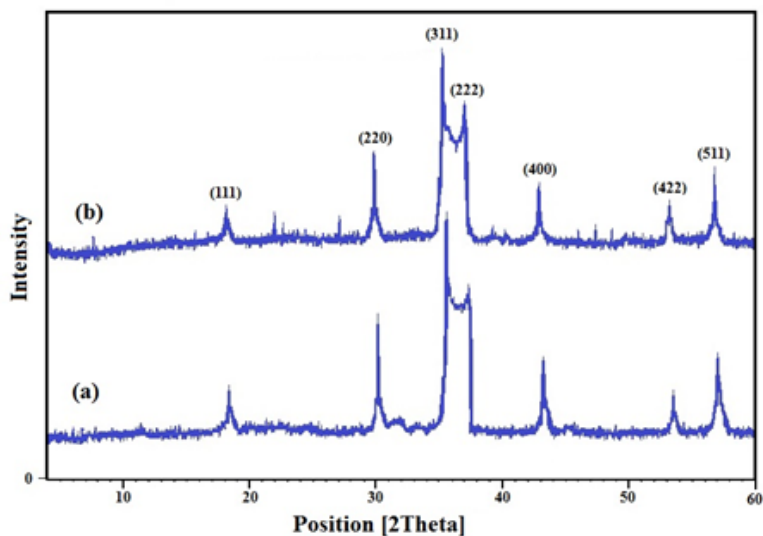


Fig. 2. XRD patterns of $\text{Ni}_{0.5}\text{Zn}_{0.5}\text{Fe}_2\text{O}_4$. (a) Synthesized $\text{Ni}_{0.5}\text{Zn}_{0.5}\text{Fe}_2\text{O}_4$; (b) standard $\text{Ni}_{0.5}\text{Zn}_{0.5}\text{Fe}_2\text{O}_4$ (JCPDS 08-0234).

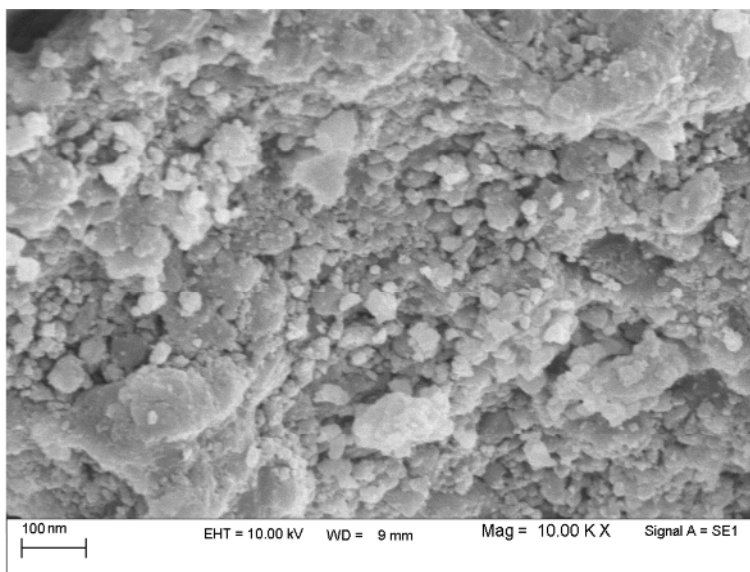


Fig. 3. SEM image of $\text{Ni}_{0.5}\text{Zn}_{0.5}\text{Fe}_2\text{O}_4/\text{M}$ nanocomposite.

Adsorption and removal of Mn (II) from aqueous solution

Effect of contact time

The effect of contact time on the amount of Mn (II) adsorbed was studied at 5 mgL^{-1} initial concentration of manganese. It could be observed from Figure 4 that with the

increase of contact time, the percentage adsorptions also increased. Minimum adsorption was 92.3% for time 5 minutes to maximum adsorption value 96.8% for the time 30 minutes. The adsorption characteristic indicated a rapid uptake of the manganese. The adsorption rate, however, reduced to a constant value with

an enhancement in contact time because of all available sites was covered, and no active site was present for adsorbing.

Effect of pH

The acidity of the aqueous solution applies a considerable effect on the adsorption process owing to it can alter the solution chemistry of contaminants and the state of functional groups on the surface of adsorbents [21-23]. The effect of solution pH on Mn (II) adsorption was studied at pH 2– 7 at 298 K. As shown in Figure 5, the adsorption rate of Mn (II) enhances with increasing pH values from 2 to 7. However, at low pH values, hydrogen ions

(H^+) were likely to compete with Mn (II) and thus lower the amount of Mn (II) removed. Therefore, the great Mn (II) adsorption occurring at higher pH could be described to a decrease in competition between H^+ and Mn (II) at the same adsorption site of the adsorbent beads. At $pH > 7$, the Mn (II) ions begin to hydrolyze and then forms insoluble manganese hydroxide. At this time, both adsorption and precipitation are to be effective mechanisms in the removal of Mn (II) ions from aqueous solution [24]. Therefore, the maximum adsorption occurs at around pH 6.0 and it is therefore selected for all adsorption experiments in this study.

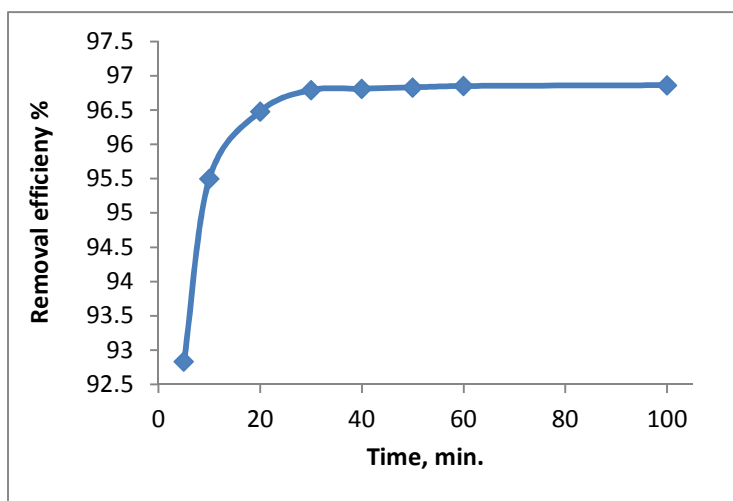


Fig. 4. Effect of contact time.

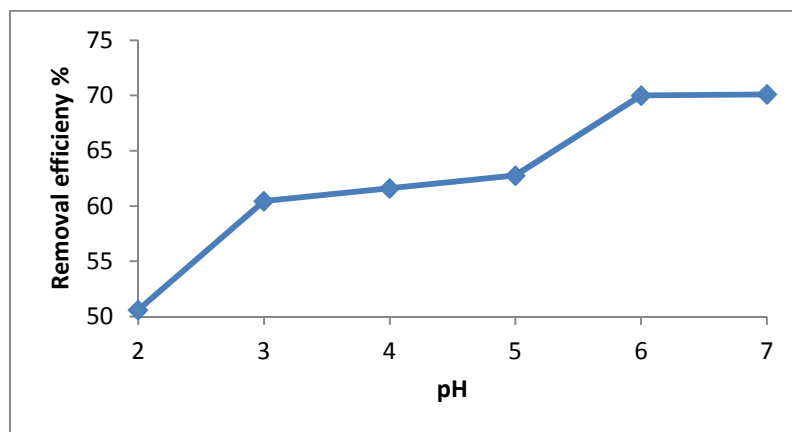


Fig. 5. Effect of pH on Mn (II).

Effect of adsorbent dosage

The effect of change in the adsorbent amount on the process adsorption of Mn (II) was investigated, with different adsorbent dose in the range of 0.01 - 0.50 g. The results obtained are shown in Figure 6. From Figure 6, it is considered that as the adsorbent dose enhances, the percentage removal also increase, until it approaches a saturation point, where the enhancement in adsorbent dose does not alter the percentage of removal. An increase in adsorption rate with adsorbent quantity can be ascribed to increased surface area and the availability of more adsorption sites. The best removal of Mn (II) is at about 88.2 %, using an adsorbent dosage of 0.30 g in 50 mL of 5 mg L⁻¹Mn (II) solution.

Effect of initial Mn (II) concentration

Batch adsorption experiments were performed at different initial Mn(II) concentrations (50, 100, 200, 300 and 600 mg L⁻¹), while other experimental parameters were constant. Figure 7 shows that adsorption capacity of Mn(II) increases, but the removal percent (%R) of Mn(II) decreases with the increase in initial concentration, indicating that the adsorption of Mn(II) on to Ni_{0.5}Zn_{0.5}Fe₂O₄/M is highly related to initial Mn(II) concentration. This observation can be described considering the fact that by increasing the initial Mn²⁺ concentration, the more Mn²⁺ ions are available, while the amount of active sites on adsorbent is constant which leads to decrease %R.

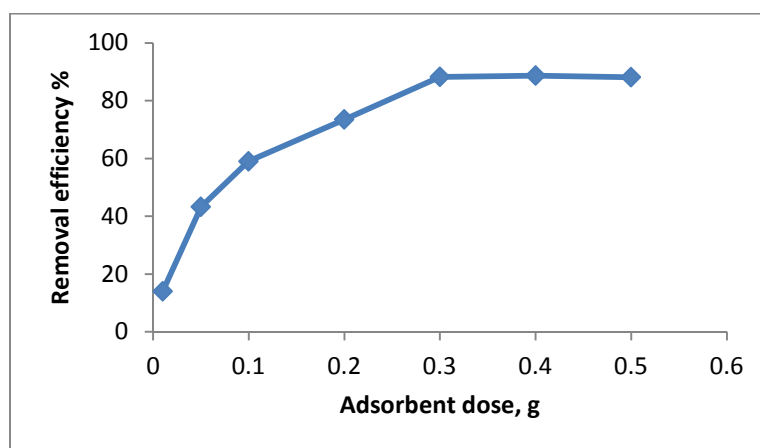


Fig. 6. The effect of adsorbent dosage.

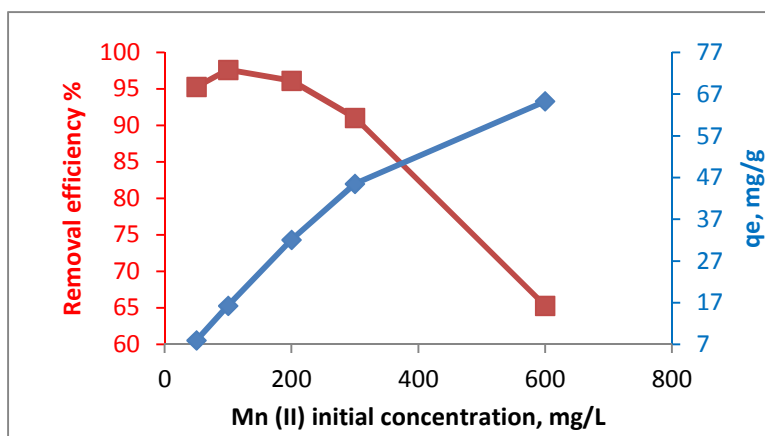


Fig. 7. Effect of initial Mn (II) concentration.

Adsorption isotherms

Isotherms study can explain how an adsorbate interacts with adsorbent. The experimental data were corresponded by Langmuir, Freundlich and Dubinin–Radushkevich models as shown in Table 1. Langmuir isotherm model, which defines a monolayer adsorption, is given in Eq. (3):

$$\frac{1}{q_e} = \frac{1}{K_L q_m} \frac{1}{C_e} + \frac{1}{q_m} \quad (3)$$

where q_e = the amount of Mn (II) adsorbed per unit mass at equilibrium (mg g^{-1});

q_m = the maximum amount of adsorbent that can be adsorbed per unit mass adsorbent (mg g^{-1});

C_e = concentration of adsorbent (in the solution at equilibrium (mg L^{-1});

K_L = adsorption equilibrium constant.

A plot of $\frac{1}{q_e}$ versus $\frac{1}{C_e}$ gives a straight line, with a slope of $\frac{1}{K_L q_m}$ and intercept $\frac{1}{q_m}$.

The main characteristics of the Langmuir isotherm can be expressed in terms of a dimensionless constant separation factor R_L that is given by Eq. (4) [25]:

$$R_L = \frac{1}{1 + K_L C_0} \quad (4)$$

where C_0 is the highest initial concentration of adsorbate (mg L^{-1}), and $K_L (\text{L mg}^{-1})$ is Langmuir constant. The value of R_L shows the shape of the isotherm to be either unfavorable ($R_L > 1$), linear ($R_L = 1$), favorable ($0 < R_L < 1$), or irreversible ($R_L = 0$). The R_L values between 0 and 1 indicate favorable adsorption. In this study, value of R_L is 0.116 shows the favorable adsorption between $\text{Ni}_{0.5}\text{Zn}_{0.5}\text{Fe}_2\text{O}_4/\text{M}$ and Mn (II).

Freundlich isotherm is expressed by Eq. (5). This isotherm model defines a heterogeneous adsorption with different surface energy sites and supposes the change of uptake with exponential distribution of adsorption sites and

energies [26-28].

$$\log q_e = \log K_F + \frac{1}{n} \log C_e \quad (5)$$

where C_e (mg L^{-1}) and q_e (mg g^{-1}) are the equilibrium concentration of adsorbent in the solution and the amount of adsorbent adsorbed at equilibrium respectively; K_F ($\text{mg}^{1-(1/n)} \text{L}^{1/n} \text{g}^{-1}$) and n are the Freundlich constant which indicate the adsorption capacity for the adsorbent and adsorption intensity, respectively.

A graph of $\log q_e$ versus $\log C_e$ provides a straight line with slope $1/n$ and intercept $\log K_F$. The value of $1/n$ mentions the adsorption intensity and the type of isotherm to be favorable ($0.1 < 1/n < 0.5$) or unfavorable ($1/n > 2$). The Freundlich parameter, $1/n$, is related to the adsorption intensity of the adsorbent. When $0.1 < 1/n \leq 0.5$, the adsorption of the adsorbate is easy; when $0.5 < 1/n \leq 1$, the adsorption process is difficult; when $1/n > 1$, adsorption takes place quite difficult [29, 30]. In our study, the value of $1/n$ (0.43) shows the favorable adsorption of Mn (II) on $\text{Ni}_{0.5}\text{Zn}_{0.5}\text{Fe}_2\text{O}_4/\text{M}$.

In order to discern between physical and chemical adsorption, the sorption data were analyzed using Dubinin–Radushkevich (D-R) equation, which is given by the Eq. (6):

$$\ln q_e = \ln q_m - \beta \varepsilon^2 \quad (6)$$

where β is a constant related to the mean energy of adsorption ($\text{mol}^2 \text{kJ}^{-2}$), q_m is the maximum adsorption capacity of metal ions (mg g^{-1}), ε is the Polanyi potential given by Eq. (7):

$$\varepsilon = RT \ln \left(1 + \frac{1}{C_e} \right) \quad (7)$$

where R is the gas constant ($8.314 \text{ J mol}^{-1} \text{ K}^{-1}$) and T is the temperature (K). By plotting $\ln q_e$ versus ε^2 with experimental data, a straight line is obtained. From the

intercept and slope, the values of q_m and β are determined. With the value of β , the mean energy E , which is the free energy transfer of one mole of solute from infinity to the surface of adsorbent, can be obtained by the Eq. (8):

$$E = \frac{1}{\sqrt{2\beta}} \quad (8)$$

For $E < 8 \text{ kJ mol}^{-1}$, the adsorption process might be performed physically, while chemical adsorption when $E > 8 \text{ kJ mol}^{-1}$ [31].

All the parameters are listed in Table 1. From Table 1, in which the Langmuir, Freundlich, D–R isotherm constants for the

adsorption of Mn (II) are summarized, it can be derived from R^2 that the Langmuir model matched the experimental data better than Freundlich and D–R models. Moreover, it is clear that the adsorption of Mn (II) by $\text{Ni}_{0.5}\text{Zn}_{0.5}\text{Fe}_2\text{O}_4/\text{M}$ may be explained as physical adsorption process for the value of E is 0.71 kJ.

The adsorption capacity is a significant parameter which determines the performance of an adsorbent. Table 2 compares the maximum adsorption capacity of $\text{Ni}_{0.5}\text{Zn}_{0.5}\text{Fe}_2\text{O}_4/\text{M}$ for Mn (II) adsorption with that of other adsorbents in the literature.

Table 1. Langmuir, Freundlich, D–R isotherm constants for the adsorption of Mn (II) ions onto $\text{Ni}_{0.5}\text{Zn}_{0.5}\text{Fe}_2\text{O}_4/\text{M}$

Langmuir			
q_m (mg g ⁻¹)	K_L	R_L	R^2
90.91	0.141	0.116	0.998
Freundlich			
1/n	K_F	R^2	
0.43	13.71	0.870	
Dubinin–Radushkevich (D–R)			
q_m (mg g ⁻¹)	β (mol ² kJ ⁻²)	R^2	E (kJ mol ⁻¹)
49.30	2×10^{-6}	0.862	0.71

Table 2 Maximum adsorption capacity of different adsorbents for Mn (II) removal

Adsorbents	q_m (mg/g)	References
Pure chitin	5.43	[32]
Rice husk	7.70	[33]
Poly(protoporphyrin-co-vinylpyridine)	5.00	[34]
Pecan nutshell	103.8	[35]
Glycine modified chitosan	71.4	[8]
Activated carbon of Ziziphusspina-christi seeds	172.41	[36]
$\text{Ni}_{0.5}\text{Zn}_{0.5}\text{Fe}_2\text{O}_4/\text{M}$	90.91	This study

CONCLUSION

$\text{Ni}_{0.5}\text{Zn}_{0.5}\text{Fe}_2\text{O}_4/\text{M}$ magnetic nanoparticles were used in adsorption of Mn (II) ions from aqueous systems and the maximum Mn (II) adsorption occurred in the pH 6 with maximum adsorption capacity of 90.91 mgg⁻¹ at 298 K. The adsorption

isotherm fitted the Langmuir model well. The prepared magnetic adsorbent can be well dispersed in the aqueous solution and easily separated from the solution with the aid of an external magnet after adsorption. The process of water treatment described

here is clean and safe using the magnetic nanoparticles. Thus, this adsorbent was found to be useful and valuable for controlling water pollution due to Mn (II) ions.

ACKNOWLEDGMENTS

The authors acknowledge the Islamic Azad University-Bandar Abbas Branch for financial support of this study.

REFERENCES

- [1]. E.-S. El-Ashtoukhy, N. Amin, and O. Abdelwahab, *Desalination* 223 (2008) 162.
- [2]. Z. Baysal, *J. Hazard Mater.* 161 (2009) 62.
- [3]. P.Senthil Kumar, *Can. J. Chem. Eng.* 91 (2013) 1950.
- [4]. Ö. Yavuz, Y., F. Güzel, *Water Res.*37 (2003) 948.
- [5]. A.A. Mengistie, T.S. Rao, A.P. Rao, *Global J. Inc.*12 (2012) 4.
- [6]. M. Suguna, *J. Chem. Pharm. Res.* 2 (2010) 7.
- [7]. J. J. ANGUILE, *Int. J. Basic Appl. Chem. Sci.*3 (2013) 7.
- [8]. K. Z. Al-Wakeel, H.A. El Monem, and M.M. Khalil, *J. Environ. Chem. Eng.*3 (2015) 179.
- [9]. Y. Shen, *Sep. Purif. Technol.*68 (2009) 312.
- [10]. D.-W. Cho, *Chem. Eng. J.*200 (2012) 654.
- [11]. G. Shi, *Sens.Actuat. B: Chem.*171 (2012) 699.
- [12]. P. Dallas, *Nanotechnology*, 17 (2006) 2046.
- [13]. D. Mohan, *Chem. Eng. J.* 172 (2011) 1111.
- [14]. S.Y. Mak, D. H. Chen., *Macromol. Rapid Commun.* 26 (2005) 1567.
- [15]. W. Nitayaphat, T. Jintakosol, *Adv. Mater. Res.*893 (2014)166.
- [16]. W. Nitayaphat, T. Jintakosol, *J. Clean. Prod.* 87 (2015) 850.
- [17]. S. Sharma, *Mater. Sci. Eng. B* 167 (2010) 187.
- [18]. A. Virden, K. O'Grady, *J. Magn. Mater.* 290 (2005) 868.
- [19]. D. Zins, V. Cabuil, R. Massart, *J. Mol. Liq.*, 83 (1999) 217.
- [20]. V. G. Pol, *Ind. Eng. Chem. Res.*49 (2009) 920.
- [21]. Y. Ren, X. Wei, M. Zhang, *J. Hazard. Mater.* 158 (2008) 14.
- [22]. Y.-T.Zhou, *J.Colloid Interf. Sci.* 330 (2009) 29.
- [23]. G. Sheng, *J. Hazard. Mater.*178 (2010) 333.
- [24]. M.A. Salam, M.S. Makki, M.Y. Abdelaal, *J. Alloy. Compd.*509 (2011) 2582.
- [25]. K.R. Hall, *Ind. Eng. Chem. Fund.* 5 (1966) 212.
- [26]. H. Chen, J. Zhao, J. Wu, G. Dai, *J. Hazard. Mater.*192 (2011) 246.
- [27]. M.-F. Hou, C. -X. Ma, W. -D. Zhang, X.-Y. Tang, Y.-N. Fan, H.-F. Wan,*J. Hazard. Mater.* 186 (2011)1118.
- [28]. Ö. Kerkez, Ş.S. Bayazit, *J. Nanoparticle Res.*16 (2014) 1.
- [29]. X.Luo, L. Zhang, *J.Hazard. Mater.* 171 (2009) 340.
- [30]. S.Samiee, E. K. Goharshadi, *J. Nanoparticle Res.* 16 (2014) 1.
- [31]. Y. Tan, M. Chen, Y. Hao, *Chem. Eng. J.* 191 (2012) 104.
- [32]. M.A. Robinson-Lora, R.A. Brennan, *Chem. Eng. J.* 162 (2010) 565.
- [33]. K.K. Krishnani, *J. Hazard. Mater.*153 (2008) 1222.
- [34]. T.F.de Oliveira, *Chem. Eng. J.* 221 (2013) 275.
- [35]. J. C. Vaghetti, *J. Hazard. Mater.* 162 (2009) 270.
- [36]. A.Omri, M. Benzina, *Alexandria Eng. J.* 51(2012) 343.

